Osteohistology of Late Triassic prozostrodontian cynodonts from Brazil

Jennifer Botha-Brink Corresp., [1, 2] , **Marina Bento Soares** [3] , **Agustín G Martinelli** [4]

[1] Karoo Palaeontology, National Museum, Bloemfontein, South Africa

[2] Department of Zoology and Entomology, University of the Free State, Bloemfontein, South Africa

[3] Departamento de Paleontologia e Estratigrafia,Instituto de Geociências, Universidade Federal do Rio Grande do Sul, Porto Alegre, Brazil

[4] Departamento de Paleontologia e Estratigrafia, Instituto de Geociências, Universidade Federal do Rio Grande do Sul, Porto Alegre, Brazil

Corresponding Author: Jennifer Botha-Brink
Email address: jbotha@nasmus.co.za

The Prozostrodontia includes a group of Triassic eucynodonts plus the clade Mammaliaformes, in which Mammalia is nested. Analysing their growth patterns is thus important for understanding the evolution of mammalian life histories. Obtaining material for osteohistological analysis is difficult due to the rare and delicate nature of most of the prozostrodontian taxa much of which comprises mostly crania or sometimes even only teeth. Here we present a rare opportunity to observe the osteohistology of several postcranial elements of the basal prozostrodontid *Prozostrodon brasiliensis*, the tritheledontid *Irajatherium hernandezi*, and the brasilodontids *Brasilodon quadrangularis* and *Brasilitherium riograndensis* from the Late Triassic of Brazil (Santa Maria Supersequence). *Prozostrodon* and *Irajatherium* reveal similar growth patterns of rapid early growth with annual interruptions later in ontogeny. These interruptions are associated with wide zones of slow growing bone tissue. *Brasilodon* and *Brasilitherium* exhibit a mixture of woven-fibered bone tissue and slower growing parallel-fibered and lamellar bone. The slower growing bone tissues are present even during early ontogeny. The relatively slower growth in *Brasilodon* and *Brasilitherium* may be related to their small body size compared to *Prozostrodon* and *Irajatherium.* These brasilodontids also exhibit osteohistological similarities with the Late Triassic/Early Jurassic mammaliaform *Morganucodon* and Late Cretaceous multituberculate mammals. This may be due to similar small body sizes, but may also reflect their close phylogenetic affinities as *Brasilodon* and *Brasilitherium* are the closest relatives to the Mammaliaformes. However, when compared with similar-sized extant placental mammals, they may have grown more slowly to adult size as their osteohistology shows it took more than one year for growth to attenuate. Thus, although they exhibit rapid juvenile growth, the small derived prozostrodontians still exhibit an extended growth period compared to similar-sized extant mammals.

Osteohistology of Late Triassic prozostrodontian cynodonts from Brazil

Jennifer Botha-Brink*[,1], Marina Bento Soares[2], and Agustín G. Martinelli[2]

[1] P. O. Box 266, Department of Karoo Palaeontology, National Museum, Bloemfontein, 9300, South Africa, and Department of Zoology and Entomology, University of the Free State, Bloemfontein, 9300, South Africa, jbotha@nasmus.co.za;

[2] Departamento de Paleontologia e Estratigrafia, Instituto de Geociências, Universidade Federal do Rio Grande do Sul, Av. Bento Gonçalves, 9500 Agronomia, 91501-970, Porto Alegre, RS, Brazil, marina.soares@ufrgs.br, agustin_martinelli@yahoo.com.ar

*Corresponding author: Jennifer Botha-Brink, Email: jbotha@nasmus.co.za

ABSTRACT

The Prozostrodontia includes a group of Triassic eucynodonts plus the clade Mammaliaformes, in which Mammalia is nested. Analysing their growth patterns is thus important for understanding the evolution of mammalian life histories. Obtaining material for osteohistological analysis is difficult due to the rare and delicate nature of most of the prozostrodontian taxa much of which comprises mostly crania or sometimes even only teeth. Here we present a rare opportunity to observe the osteohistology of several postcranial elements of the basal prozostrodontid *Prozostrodon brasiliensis*, the tritheledontid *Irajatherium hernandezi*, and the brasilodontids *Brasilodon quadrangularis* and *Brasilitherium riograndensis* from the Late Triassic of Brazil (Santa Maria Supersequence). *Prozostrodon* and *Irajatherium* reveal similar growth patterns of rapid early growth with annual interruptions later in ontogeny. These interruptions are associated with wide zones of slow growing bone tissue. *Brasilodon* and *Brasilitherium* exhibit a mixture of woven-fibered bone tissue and slower growing parallel-fibered and lamellar bone. The slower growing bone tissues are present even during early ontogeny. The relatively slower growth in *Brasilodon* and *Brasilitherium* may be related to their small body size compared to *Prozostrodon* and *Irajatherium*. These brasilodontids also exhibit osteohistological similarities with the Late Triassic/Early Jurassic mammaliaform *Morganucodon* and Late Cretaceous multituberculate mammals. This may be due to similar small body sizes, but may also reflect their close phylogenetic affinities as *Brasilodon* and *Brasilitherium* are the closest relatives to the Mammaliaformes. However, when compared with similar-sized extant placental mammals, they may have grown more slowly to adult size as their osteohistology shows it took more than one year for growth to attenuate. Thus, although they

exhibit rapid juvenile growth, the small derived prozostrodontians still exhibit an extended growth period compared to similar-sized extant mammals.

INTRODUCTION

The Prozostrodontia is a group of Late Triassic probainognathian eucynodonts (Liu and Olsen, 2010), which includes Mammaliaformes and crown Mammalia in its definition. The non-mammaliaform prozostrodontians illustrate the ~~prior steps~~ to the rise of Mammaliaformes, and they are thus~~,~~ important for understanding the origin and evolution of mammals. The Prozostrodontia contain several unranked taxa (e.g., *Prozostrodon*, *Therioherpeton*, *Alemoatherium*, *Botucaraitherium*), as well as two well-known major clades, the Tritylodontidae and Tritheledontidae, both closely related to the Mammalia (Liu and Olsen, 2010; Soares, Martinelli and Oliveira, 2014, Martinelli et al., 2017a, b). The Tritylodontidae ~~(basal skull length, BSL ~50–250 mm)~~ are a group of highly specialized herbivorous prozostrodontians that arose during the Late Triassic and went extinct during the Early Cretaceous (e.g., Clark and Hopson, 1985; Sues, 1986; Matsuoka, Kusuhashi and Corfe, 2016). The Tritheledontidae are a group of small (BSL ~30–70 mm), faunivorous/frugivorous forms that existed from the Late Triassic to Early Jurassic (Kemp, 2005; Gow, 1980; Martinelli et al., 2005; Martinelli and Rougier, 2007; Soares, Schultz and Horn, 2011). There has been much debate regarding which group is more closely related to mammals as both groups have derived cranial and postcranial features typical of Mammaliaformes that reveals different topologies according to different phylogenetic hypotheses (e.g., Luo, 1994; Hopson and Kitching, 2001; Kemp, 2005; Abdala, 2007).

However, more recently discovered taxa from Brazil (i.e., *Brasilodon quadrangularis*, *Brasilitherium riograndensis*, *Minicynodon maieri*, *Botucaraitherium belarminoi*; Bonaparte et al., 2003, 2010; Bonaparte, Martinelli and Schultz, 2005; Bonaparte, Soares and Martinelli, 2012; Soares, Martinelli and Oliveira, 2014) show a closer relationship to Mammaliaformes than the aforementioned groups (Bonaparte, Martinelli and Schultz, 2005; Soares, Martinelli and Oliveira, 2014; Martinelli et al., 2017a, b). Some of these species were grouped into Brasilodontidae (Bonaparte, Martinelli and Schultz, 2005), but their monophyly and composition (e.g., Bonaparte, 2013) should be tested more comprehensively, as well as the taxonomic validity of some of the members (see Liu and Olsen, 2010; Martinelli and Bonaparte, 2011; Martinelli, 2017). These tiny (BSL approximately ~20–55 mm) faunivorous/frugivorous animals lived during the Late Triassic and have a set of derived features (e.g., "triconodont"–like dentition, lack of a postorbital bar, slender horizontal ramus of the dentary and zygomatic arch, petrosal with a promontorium) that is not seen in any other non-mammaliaform cynodont, making them important taxa for understanding the early evolution of Mammaliaformes (Kemp, 2005; Bonaparte, Martinelli and Schultz, 2005; Bonaparte, Soares and Martinelli, 2012; Bonaparte, 2013; Rodrigues, Ruf and Schultz, 2013, 2014).

The South American prozostrodontians and closely related forms (e.g., *Protheriodon*, *Candelariodon*) are particularly noteworthy as several important finds have shed light on the morphological changes that occurred prior to and during the evolution of the Mammaliaformes (Bonaparte and Barberena, 2001; Bonaparte, Martinelli and Schultz, 2005; Soares, Schultz and Horn, 2011; Rodrigues, Ruf and Schultz, 2013; Martinelli, Bento Soares and Schwanke, 2016; Martinelli et al., 2017a, b). This remarkable record includes about 20 species of probainognathians (ecteniniids, chiniquodontids, probainognathids and prozostrodontians) from

Brazil and Argentina in a fairly continuous span of ~8 million years (Abdala and Ribeiro, 2010; Martinelli and Soares, 2016). Among prozostrodontians, many taxa are tiny with some having basal skull lengths of only 20–40 mm (e.g. *Minicynodon*, *Brasilodon*, *Brasilitherium*) (Bonaparte et al., 2010; Martinelli, Bento Soares and Schwanke, 2016). Given that they are so small and delicate, the best represented elements are jaws and teeth, with only a few partial and/or complete skulls and very ~~little~~ associated postcranial bones. Postcranial material can provide insight into various aspects of the biology of these taxa, such as body size, biomechanics and life history. Life history data, such as ontogenetic status, habitat preference, growth patterns and rates, can be obtained by assessing the bone microstructure or osteohistology of limb bones, and provides novel information that may not necessarily be gained from studying the gross morphology.

We describe here the limb bone osteohistology of four Late Triassic Brazilian non-mammaliaform prozostrodontian taxa. We assess their life histories and compare their growth patterns with those of less derived eucynodonts and more derived Mammaliaformes, thus filling a knowledge gap in the cynodont-mammal transition.

MATERIAL AND METHODS

Institutional Abbreviations

UFRGS-PV-T- Universidade Federal do Rio Grande do Sul, Brazil, Paleovertebrates Collection, Triassic.

Material

Our sample comprises *Prozostrodon brasiliensis* (estimated BSL ~75–80 mm), which is one of the most basal prozostrodontians (Bonaparte and Barberena, 2001; Liu and Olsen, 2010; Martinelli, Bento Soares and Schwanke, 2016), the tritheledontid *Irajatherium hernandezi* (Martinelli et al., 2005; Oliveira, Martinelli and Bento Soares, 2011) (estimated maximum BSL 80 mm), and the brasilodontids *Brasilodon quadrangularis* and *Brasilitherium riograndensis* (both with a maximum estimated BSL of 40 mm). The BSLs of *Brasilodon* and *Brasilitherium* are taken from specimens that were assigned to each of these taxa by Bonaparte (2013), Bonaparte, Martinelli and Schultz (2005) and Bonaparte, Soares and Martinelli (2012). However, Liu and Olsen (2010) and Martinelli and Bonaparte (2011) suggested that these two taxa should be synonymised and that the specimens of both taxa represent different ontogenetic stages of one taxon (see also Martinelli, 2017). With the exception of one specimen (UFRGS-PV 1043; Bonaparte et al., 2010; Bonaparte, Soares and Martinelli, 2012, used also in other contributions), most specimens referred to *Brasilitherium* are small-sized compared to the *Brasilodon* ones. Some authors have maintained the use of both taxa in their analyses (e.g., Bonaparte, 2013; Martinelli et al., 2017a, b), but studies are currently being undertaken (AGM, MBS) that will shed light on this issue. A consensus has yet to be reached and thus, the taxa are treated separately here, with the caveat that the osteohistology of these two taxa may be shown to represent one species in the future.

The material of *Prozostrodon brasiliensis* includes a proximal portion of a left humerus and complete left femur of the holotype UFRGS-PV-0248-T (the only known specimen with postcranial material). UFRGS-PV0-248-T was found 200 m northwest of the Cerriquito Hill, in a road cut on highway BR-287, in the municipality of Santa Maria, Rio Grande do Sul State, Brazil (Bonaparte and Barberena, 2001). It comes from the *Hyperodapedon* Assemblage Zone

(AZ) of the Candelária Sequence (Horn et al., 2014), Santa Maria Supersequence (Zerfass et al., 2003), which is considered to be Late Carnian in age based on biostratigraphical correlations with the Ischigualasto Formation of Argentina (e.g., Langer, 2005).

The material of *Irajatherium hernandezi* comprises an almost complete humerus (with only the proximal end missing) (UFRGS-PV-1072-T), which was described by Oliveira, Martinelli and Bento Soares (2011). The material of *Brasilodon quadrangularis* consists of the shaft of an ulna (the articular proximal portion was preserved separately) associated with a skull and jaws (UFRGS-PV-765-T). It was figured in Bonaparte, Martinelli and Schultz (2005:fig. 6). The *Brasilitherium riograndensis* material consists of two specimens: UFRGS-PV-1308-T (small-sized specimen), preserved in a sandstone block with a radius, ulna, femur, tibia, and fibula (associated with a lower jaw and maxilla referred to *Brasilitherium*, which has not been formally published); UFRGS-PV-1043-T (large-sized specimen), a proximal portion of the left femur, which is associated with a skull, jaws and other postcranial elements (e.g., Bonaparte et al., 2010; Bonaparte, Soares and Martinelli, 2012; Rodrigues, Ruf and Schultz, 2013, 2014; Ruf et al., 2014).

All the specimens of *Irajatherium*, *Brasilitherium* and *Brasilodon* come from the outcrop known as Linha São Luiz Site, located approximately 3 km north of Faxinal do Soturno city, Rio Grande do Sul State, Brazil. They come from the *Riograndia* AZ (above the *Hyperodapedon* AZ) of the Candelária Sequence (Horn et al., 2014), Santa Maria Supersequence (Zerfass et al., 2003), of Late Carnian-Early Norian age based on biostratigraphical correlation with the Ischigualasto and Los Colorados formations of Argentina (e.g., Martínez et al., 2013; Martinelli, Bento Soares and Schwanke, 2016).

Methods

All the elements were measured and photographed prior to thin sectioning. Although mostly fragmentary material was thin sectioned (given the rarity of the taxa), all the bones were associated with diagnostic cranial material. The elements were serially sectioned where possible, but some of the bones were so small than only one or two sections could be recovered from each bone. The thin sectioning process was conducted at the National Museum, Bloemfontein, South Africa. The bones were embedded in the clear Struers Epofix epoxy resin under vacuum. Once set, the resin blocks were serially sectioned using a Struers Accutom-100 cutting and grinding machine. Each thick section was adhered to a frosted glass slide using the Struers Epofix resin. These sections were then ground to a thickness of approximately 60 μm using the Struers Accutom-100 and polished manually using Struers Accutom-100 cutting oil. The resulting thin sections were then digitally rendered under ordinary, polarized (PL), and cross-polarized light (CPL), using a Nikon Eclipse Ci POL polarizing microscope and DS-Fi3 digital camera in NIS-Elements 4.6 (Nikon Corp.). Osteohistology terminology follows that of Francillon-Vieillot et al. (1990) and Ricqlès et al. (1991).

RESULTS

Prozostrodon brasiliensis

A left humerus (UFRGS-PV248a-T) comprising the proximal midshaft (the region of the deltopectoral crest) and epiphysis was thin sectioned (Fig. 1A–C). In transverse section, the bone contains a relatively small medullary cavity surrounded by a thick compact cortex (Fig. 1A). A few thick bony trabeculae traverse the otherwise clear medullary cavity. Several large resorption cavities in the perimedullary region are surrounded by thick layers of endosteal lamellae. A few

of these resorption cavities extend into the area of the deltopectoral crest. Small secondary osteons, demarcated by their cement lines, are rare and limited to the innermost cortex in the midshaft, but are more abundant in the metaphyseal region. The compact cortex is comprised of a woven-fibered matrix with abundant, large, globular, haphazardly arranged osteocyte lacunae and numerous vascular canals (Fig. 1B, C) forming a fibrolamellar bone tissue complex (defined by the presence of a woven-fibered bone matrix associated with primary osteons; Francillon-Vieillot et al., 1990). Most of the canals form poorly developed longitudinally-oriented primary osteons in radial rows, but some radiate transversely, particularly in the region of the deltopectoral crest, and others a reticular pattern, especially at the bone periphery, further down the midshaft. The fibrolamellar bone is interrupted by two regions of parallel-fibered bone tissue (Fig. 1B). The first is a thick region (16 μm) of less vascularized parallel-fibered bone tissue midway through the cortex. The osteocyte lacunae are more uniformly distributed in this region (i.e. there is no evidence of static osteogenesis; Stein and Prondvai, 2013). The parallel-fibered bone matrix becomes increasingly organized within its center to form lamellar bone with flattened osteocyte lacunae arranged parallel to one another. A LAG (Fig. 1A, B), which becomes an annulus in parts (Fig. 1C), indicating a temporary cessation or decrease in growth rate respectively, traverses the middle of this slower growing region. A thin zone of more vascularized fibrolamellar bone follows from this region, which is then followed by a second, thinner region (7 μm) of parallel-fibered bone in the outer cortex. The bone tissue returns to highly vascularized fibrolamellar bone at the subperiosteal surface with a reticular or radiating vascular network, showing that the bone was still actively growing at the time of death. Sharpey's fibers, indicating areas of muscle attachment, were observed in the proximal

metaphysis on the dorsal side of the bone (Fig. 1C), possibly for the insertion of the *latissimus dorsi* or *teres minor* muscles (Jenkins, 1971).

In transverse section, the left femur (UFRGS-PV-248b-T) comprises a small medullary cavity surrounded by a thick compact cortex (Fig. 1D). The medullary cavity is completely clear and is only traversed by a few thick broken trabeculae further away from the midshaft. Several large resorption cavities can be found in the perimedullary region. Secondary osteons are small and rare, and limited to the innermost cortex, similar to the humerus. The compact cortex is similar to the humerus, i.e. it comprises highly vascularized fibrolamellar bone with mostly short radiating vascular canals and longitudinally-oriented primary osteons in the inner cortex and short radiating canals at the subperiosteal surface (Fig. 1D), which become more reticular further down the midshaft (Fig. 1E, F). The fibrolamellar bone is also interrupted by parallel-fibered bone tissue (10 µm thick) midway through the cortex, similar to the humerus. It appears as two regions in some areas (similar to the humerus), but merges to form one zone in others. A LAG (Fig. 1D), which becomes an annulus in parts (Fig. 1E, F), can be seen running through parts of this region. Rapid growth resumes after this slow growing region in the form of rapidly growing fibrolamellar bone, indicating active growth at the time of death. Sharpey's fibers, indicating areas of muscle insertion, were observed on the dorsomedial and ventrolateral sides of the midshaft, possibly for the origin of the femoro-tibialis and adductor muscles, respectively, as well as on the ventral side of the proximal epiphysis (Fig. 1G), possibly for the insertion of the ilio-femoralis or adductor muscles (Jenkins, 1971). The femoral longitudinal sections reveal a similar bone tissue pattern to the transverse sections. The vascular canals in both proximal and distal epiphyses stop just beneath the bone surfaces, which are themselves capped by a thin layer of calcified cartilage.

229

230 ***Irajatherium hernandezi***

231 The midshaft and distal end of a left humerus (UFRGS-PV-1072-T) was available for thin
232 sectioning (Fig. 2A–D). The bone tissues are not particularly well preserved and appear to have
233 been infiltrated with some kind of mineral. However, although parts appear to be diagenetic, the
234 main features of the bone tissue can be clearly observed from several well preserved patches of
235 primary bone. In transverse section, the bone comprises a small medullary cavity traversed by a
236 few thick trabeculae (Fig. 2A). Secondary remodeling is limited to a few small secondary
237 osteons in the inner cortex. The surrounding thick, compact cortex consists of an inner cortex of
238 fibrolamellar bone with mostly longitudinally-oriented primary osteons (in radiating rows in a
239 few patches) and a few short radiating canals (Fig. 2B, C). The outer third of the cortex gives
240 way to parallel-fibered bone and in places lamellar bone (Fig. 2A), with more uniformly
241 distributed osteocyte lacunae. At least one LAG (Fig. 2A) is present in this thick region, but
242 there looks like there may be more (Fig. 2B, D). Confirmation is difficult, however, as the
243 diagenesis appears to have highlighted the individual lamellae of the bone tissue. This would
244 then suggest the presence of lamellar bone, where the individual layers of this bone tissue type
245 have been highlighted by the mineral infiltration, and indicates slow bone deposition. The
246 osteocyte lacunae density is lower and their distribution more uniform (Fig. 2D) compared to
247 that seen in the inner and mid-cortex (Fig. 2C). The distal longitudinal sections revealed similar
248 bone tissue patterns to the midshaft, but there are clearer views of numerous, large, globular
249 osteocyte lacunae in the metaphysis, possibly as a result of ongoing bone activity during
250 remodeling in this area.

Despite the uncertain number of LAGs, the features listed above do indicate a transition to slower growth. The slow growing zone may indicate an External Fundamental System (EFS), which is generally demarcated by several closely spaced growth marks and/or the onset of slow growing tissue at the subperiosteal surface. An EFS would indicate that growth had essentially ceased, but the presence of vascular canals within the slower growing region, as well as at the subperiosteal suggests that the bone was still growing (although more slowly) and that maximum size had yet to be reached. Although not fully grown, however, this individual was no longer a juvenile as the overall growth rate had decreased indicating that it was a subadult that had reached the growth deceleration phase.

Brasilodon quadrangularis

The ulna of *Brasilodon* (UFRGS-PV-765-T) contains a large clear medullary cavity surrounded by a thin compact cortex (Fig. 3A). A thin layer of endosteal bone with flattened, parallel osteocyte lacunae lines the medullary cavity on the medial side of the bone. The bone tissue consists of patches of woven-fibered bone with large, globular, haphazardly arranged osteocyte lacunae and a few poorly developed tiny primary osteons (Fig. 3B, C). There is a peripheral region on the medial side, however, that contains a few flattened osteocyte lacunae and differs in color from the rest of the cortex under cross polarized light. This region of lamellar bone may represent an annulus (Fig. 3D). A few tiny secondary osteons could be observed within the olecranon process (Fig. 3A).

Brasilitherium riograndensis

The radius, ulna, femur, tibia and fibula of the smaller individual of *Brasilitherium* were thin sectioned (UFRGS-PV-1308-T). The radius (UFRGS-PV-1308a-T) contains a large clear medullary cavity surrounded by poorly vascularized parallel-fibered bone (Fig. 4A). The osteocyte lacunae are globular, but arranged uniformly throughout the cortex. The vascular canals are all tiny and simple. Neither primary nor secondary osteons are present. There is no change in tissue type towards the subperiosteal surface and growth marks are absent.

The ulna (UFRGS-PV-1308b-T) has a very large clear medullary cavity and thin compact cortex. The bone tissues are simple, similar to the radius, but the flattened, parallel osteocyte lacunae indicate the presence of lamellar bone instead of parallel-fibered bone. In some patches, the individual lamellae can be clearly seen. Vascularization is simple, similar to the radius, although slightly more vascularized. One lamella, towards the subperiosteal surface, appears to be more prominent than the others, and is different in color under cross-polarized light compared to the other lamellae (Fig. 4B). It may represent a LAG, but this cannot be confirmed as it only appears in one corner of the bone.

The femur of this same individual (UFRGS-PV-1308c-T) also contains a large, free medullary cavity and thin cortex (Fig. 4C). A few broken bony trabeculae were observed in the center of the cavity. The bone tissue contains a mixture of types, ranging from woven-fibered to parallel-fibered to lamellar in various regions (Fig. 4C, D). Some tiny patches contain globular, haphazardly arranged osteocyte lacunae and a few tiny, poorly developed primary osteons, indicating fibrolamellar bone. Other areas contain more organized osteocyte lacunae some of which are flattened, indicating parallel-fibered and lamellar bone. In these regions, the vascular canals are simple. Although, not highly vascularized, the canals are more abundant than the radius and ulna. There is no evidence of a decrease in vascularization at the subperiosteal surface

296 indicating continued growth. A few tiny secondary osteons were observed in the innermost
297 cortex. Growth marks were not observed.

298 The tibia (UFRGS-PV-1308d-T) is similar to the femur, with a large open medullary
299 cavity and a mixture of bone tissue types in the compact cortex (Fig. 4E). Patches of woven-
300 fibered bone with a few primary osteons (Fig. 4F) indicating the presence of poorly developed
301 fibrolamellar bone, is mixed with areas of parallel-fibered bone. One tiny secondary osteon was
302 observed in the outer cortex. Growth marks are absent.

303 The fibula (UFRGS-PV-1308e-T) contains an open medullary cavity and a relatively
304 thick cortex. The compact cortex comprises primarily avascular lamellar bone tissue (Fig. 4G).
305 There is a patch of globular osteocyte lacunae towards the end of the bone in the region of the
306 metaphysis. A few small vascular canals are also present in this region. The osteocyte lacunae
307 are a mixture of both globular and flattened bodies. Growth marks were not observed.

308 The larger femur (UFRGS-PV-1043-T) from the second *Brasilitherium* individual also
309 contains a large free medullary cavity and relatively thin cortex (Fig. 4H–J). One large resorption
310 cavity was observed towards the direction of the greater trochanter, otherwise secondary
311 remodeling is limited to a few tiny secondary osteons in the innermost cortex. There are small
312 patches of woven-fibered bone with haphazardly arranged osteocyte lacunae in the inner cortex,
313 but they become increasingly uniformly distributed towards the subperiosteal surface to form
314 parallel-fibered bone and even lamellar bone in places (Fig. 4I). Vascularization is moderate and
315 comprises some small longitudinally-oriented primary osteons and simple canals. A LAG runs
316 through the mid-cortex on the posterior side of the bone, although it should be noted that it
317 cannot be traced around the whole bone. There is no evidence of an EFS, but the increased
318 prevalence of parallel-fibered bone at the subperiosteal surface suggests an overall decrease in

growth rate and a departure from the juvenile stage. Although not fully grown, this individual was likely a subadult when it died.

DISCUSSION

Prozostrodon brasiliensis represents one of the most basal members of the Prozostrodontia (Liu and Olsen, 2010; Martinelli et al., 2017a, b) and provides a good example of the type of growth patterns that existed during the early evolution of this clade. The presence of well vascularized rapidly forming fibrolamellar bone is similar to that found in all other non-mammaliaform cynodonts, including one of the most basal cynodonts, *Procynosuchus*, which exhibits fibrolamellar bone during the early stages of ontogeny (Botha-Brink, Abdala and Chinsamy, 2012). The temporary decrease and cessation in growth shows that *Prozostrodon* grew cyclically as did most of the gomphodont cynodonts (Botha-Brink, Abdala and Chinsamy, 2012). The vascular pattern in the bone tissues of *Prozostrodon*, with the high incidence of longitudinally-oriented primary osteons, compares well with the Early Jurassic tritylodontid *Tritylodon longaevus* (Botha-Brink, Abdala and Chinsamy, 2012), although the reticular patches are also similar to the Early Triassic basal epicynodont *Thrinaxodon liorhinus* (Botha-Brink, Abdala and Chinsamy, 2012). It is clear from the highly vascularized, rapidly deposited bone tissues that *Prozostrodon* grew quickly during the favorable growing season. The expansive width of the slow growing parallel-fibered zone is noteworthy, however, as this differs from the gomphodonts that have been studied to date (i.e. *Diademodon*, *Trirachodon*, *Langbergia*, *Andescynodon*, *Traversodon*, *Gomphodontosuchus*, *Protuberum*, *Scalenodontoides*, *Exaeretodon*; Botha and Chinsamy, 2000, 2004; Chinsamy and Abdala, 2008; Botha-Brink, Abdala and Chinsamy, 2012; Veiga, Botha-Brink and Soares, 2018), which all express LAGs or narrow annuli of parallel-

342 fibered or lamellar bone. The broadness of this slow growing zone indicates that either the
343 animal was able to continue growing through much of the cold or dry season, only ceasing when
344 the LAG was deposited, or that it experienced a particularly long and harsh unfavorable growing
345 season and thus, grew slowly for longer under these conditions.

346 Although UFRGS-PV248-T is the largest known specimen of *Prozostrodon*, the presence
347 of continued active rapid growth at the periphery of the bones indicates that it was not a mature
348 individual. There is no overall deceleration in growth and thus, it had not likely attained
349 reproductive maturity before it died. A deceleration in growth rate typically accompanies the
350 onset of reproductive maturity in extant mammals that take several years to reach a large body
351 size (Owens, Dubeski and Hanson, 1993; Köhler et al., 2012), but may occur after asymptotic
352 size is reached in fast growing very small mammals (e.g. the long-clawed shrew, Nesterenko and
353 Ohdachi, 2001; grey mouse lemur, Castanet et al., 2004) or prior to this transition in very large
354 taxa (e.g. elephant, Lee and Werning, 2008). Although the maximum known BSL of
355 *Prozostrodon*, which is 80 mm, does not represent a fully grown individual, the taxon is not
356 likely to have reached the large body sizes of extant mammals that take several years to reach
357 reproductive maturity, such as ruminants (two to four years), the hippopotamus (10 years) or
358 elephant (15 years) (Miller and Zammuto, 1983; Promislow and Harvey, 1990; Köhler et al.,
359 2012). *Prozostrodon* falls within the size range of small extant mammals that typically attain
360 reproductive maturity within one year (Miller and Zammuto, 1983; Promislow and Harvey,
361 1990). However, given the mid-cortical growth mark in the *Prozostrodon* material and continued
362 rapid growth, it is likely that this taxon took longer than one year to become reproductively
363 mature.

To date, *Irajatherium hernandezi* is the only tritheledontid cynodont ~~where the~~ limb bones have been studied histologically. The bone tissues revealed rapidly forming fibrolamellar bone with similar vascular arrangements to that seen in *Tritylodon* (Botha-Brink, Abdala and Chinsamy, 2012). Although the material is poorly preserved, peripheral interruptions in growth (at least one LAG) can be clearly seen. The presence of vascular canals at the subperiosteal surface indicates that growth continued, but the canals are fewer and smaller compared to those in the mid and inner cortex and a slower forming tissue (lamellar bone) appears in this region, indicating a decrease in growth rate. The presence of at least one LAG, however, indicates that growth was cyclical. Botha-Brink, Abdala and Chinsamy (2012) suggested that *Tritylodon* generally grew in a sustained manner as growth marks were rarely found in the material studied, but the presence of a double LAG in a radius and fibula belonging to specimen BP/1/5167 indicates that *Tritylodon* was capable of cyclical growth. Upon further investigation it was found that much of the *Tritylodon* material that has been thin sectioned represents juveniles and the presence of continued growth after the LAG in the bones of BP/1/5167 indicates that it was just over a year old at the time of death and not fully grown (JBB pers. obs. 2018). However, the *Irajatherium* material reveals that a slower growth phase had been reached and thus, was not likely to have grown significantly larger than the maximum known BSL of 80 mm. This suggests that it was a smaller taxon than *Tritylodon* (maximum known BSL 140 mm and an estimated body mass of 10 kg; Gaetano, Abdala and Govender, 2017) or *Prozostrodon*. It is interesting that despite the smaller body size, the bone tissues of *Irajatherium* still show rapid growth rates as smaller taxa within a given clade tend to grow more slowly than their larger bodied relatives (Case, 1978).

Among the small-sized prozostrodontians from South America, *Irajatherium* is the only one in which fossorial features in the humerus have been recognized (Martinelli et al., 2005). This taxon has a stout humerus, with twisted and broad proximal and distal epiphyses, a proximally deep ~~biccipital~~ groove, and two well-developed processes for the ~~T~~eres major muscle (Martinelli et al., 2005; Oliveira, Martinelli and Bento Soares, 2011). The osteohistology revealed a relatively thick cortex where the compact bone wall (cortical thickness) comprises 29% of the bone diameter. Similarly thick cortices have been found in extant burrowing mammals such as *Heterocephalus glaber* (naked mole rat, 31%) and *Erethizon* (~~new world~~ porcupine >30%), as well as the burrowing or digging lizards *Gerrhonotus grantis*, *Heloderma suspectum* and *Phrynosoma douglassi* (Magwene, 1993; Botha and Chinsamy, 2004). A thick, robust humerus would have aided in counteracting strong bending forces during forelimb digging. Interestingly, *Prozostrodon* also has relatively thick cortices (humerus 30%, femur 35%), but no fossorial adaptations can be identified in the limb bones of this taxon. The thick cortices may be attributed to a larger body size compared to *Irajatherium*.

The bone tissues of *Brasilodon* and *Brasilitherium* are similar, with a mixture of woven and parallel-fibered bone tissues. If we place all of our brasilodontid study material in an ontogenetic series: the *Brasilitherium* UFRGS-PV-1308-T individual is the smallest, with *Brasilodon* UFRGS-PV-765-T being larger and *Brasilitherium* UFRGS-PV-1043-T the largest individual in the series. This is supported by the osteohistology analysis. The bones of the smallest *Brasilitherium* UFRGS-PV-1308-T contain a mixture of rapidly forming woven-fibered bone and slower growing parallel-fibered bone. The absence of any growth marks or an EFS suggests that this individual was in an early ontogenetic stage (within its first year) at the time of death. The bone tissues of *Brasilodon* UFRGS-PV-765-T also contain a mixture of woven-

409 fibered bone and parallel-fibered bone, but there appears to be an annulus at the bone periphery,
410 suggesting that it was ontogenetically older (it had reached its first year) than the small
411 *Brasilitherium* UFRGS-PV-1308-T. The larger *Brasilitherium* UFRGS-PV-1043-T contains a
412 LAG with continued growth after this growth mark, suggesting that it was ontogenetically older
413 than the *Brasilodon* individual. It is recognized that our sample size is very small and more
414 material is required for osteohistology to be used as supportive evidence for the synonymy of
415 these two taxa. However, it is worth noting that there is no evidence in the study material to
416 contradict the possibility that *Brasilodon* and *Brasilitherium* are synonymous and that they may
417 represent different ontogenetic stages in a series (see also Liu and Olsen, 2010; Martinelli and
418 Bonaparte, 2011; Martinelli, 2017).

419 The presence of a mid-cortical LAG in the largest *Brasilitherium* individual (UFRGS-
420 PV-1043-T), prior to the onset of the slower forming peripheral parallel-fibered bone, suggests
421 that this taxon took longer than one year to reach somatic or reproductive maturity. Thus,
422 although it was a tiny species and capable of growing quickly (given the presence of rapidly
423 forming woven-fibered bone), it still took longer than one year to reach asymptotic size. This
424 contrasts to what is seen in similar-sized extant mammals (e.g. rodents; Nesterenko and Ohdachi,
425 2001).

426 Comparing the brasilodontids with mammaliaforms is difficult because the only
427 mammaliaform that has been sectioned is the tiny (BSL 30 mm, Kemp, 2005) Early Jurassic
428 *Morganucodon watsoni* (Chinsamy and Hurum, 2006) and the sections are poorly preserved.
429 Chinsamy and Hurum (2006) identified a patch of woven-fibered bone and noted some
430 peripheral parallel-fibered bone tissue with LAGs in their *Morganucodon* sample, but much of
431 the material is diagenetic. There is another section of a *Morganucodon* ulna in the National

Museum of Natural History (Paris, France), but it is also badly preserved and little information can be obtained from the sample (JBB pers. obs. 2015). Given that Chinsamy and Hurum (2006) noted a mixture of woven-fibered and parallel-fibred bone, it appears that it grew in a similar manner to the brasilodontids. However, O'Meara and Asher (2016) proposed that *Morganucodon* grew more similarly to extant placental mammals than did more basal non-mammaliaform cynodonts because it exhibits a truncated growth period, with rapid juvenile growth and a very short period of adult growth. The narrow range of skull lengths in *Morganucodon* supports their proposal where rapid attainment of somatic maturity would restrict size variation (O'Meara and Asher, 2016). The skull length variation of *Brasilodon* and *Brasilitherium* (BSL ranging from 20–40 mm) exceeds that of the known samples of *Morganucodon* (Luo, Crompton and Sun, 2001; O´Meara and Asher, 2016). Combined with the osteohistology results, it suggests that the Brazilian non-mammaliaform cynodonts had a more protracted growth period where, although juvenile growth was rapid, they still took longer to reach somatic maturity than did *Morganucodon*.

Interestingly, *Brasilodon* and *Brasilitherium* grew more quickly than the similar-sized Late Cretaceous eutherian mammals *Barunlestes butleri* (BSL approximately 30 mm, Kielan-Jaworowska, Cifelli and Luo, 2004) and *Zalambdalestes lechei* (BSL approximately 50 mm, Kielan-Jaworoswka, Cifelli and Luo, 2004). Contrary to the brasilodontids, the bones of these eutherians are composed entirely of very poorly vascularized lamellar-zonal bone, indicative of slow growth (Chinsamy and Hurum, 2006). Given that all these taxa were similar in body size, the differences in growth cannot be attributed to differences in size. Instead, the brasilodontids exhibit similar bone tissues and growth patterns to the Late Cretaceous multituberculates *Kryptobaatar dashzevegi* (BSL approximately 30 mm, Kielan-Jaworowska, 1970) and

455 *Nemegtbaatar gobiensis* (BSL approximately 45 mm, Kielan-Jaworowska, 1974). Chinsamy and
456 Hurum (2006) found woven-fibered bone in a *Kryptobaatar* femur, indicating rapid growth, but
457 the absence of an EFS or any change in growth rate near the sub-periosteal surface indicates that
458 it was still a young individual at the time of death and thus, does not contain a complete growth
459 record of the animal. The femur of *Nemegtbaatar* contains parallel-fibered bone and a LAG,
460 indicating slightly slower cyclical growth. Both bone tissue types and growth marks were
461 observed in the brasilodontids, suggesting a closer similarity in growth pattern to the
462 multituberculates than to the eutherian mammals *Barunlestes* and *Zalambdalestes.* Sampling
463 more early eutherians and other Mesozoic mammal lineages, however, will provide a more
464 conclusive assessment of the growth patterns of stem and early crown mammals.
465
466 **Implications for non-mammaliaform cynodont physiology**
467 The presence of rapidly forming fibrolamellar bone in even the most basal therapsids (e.g.
468 dinocephalians; Shelton and Chinsamy, 2016) shows that high growth rates were present prior to
469 the evolution of the non-mammaliaform cynodonts. Dicynodont, gorgonopsian and
470 therocephalian therapsids dominated the terrestrial landscape during the Late Permian, growing
471 rapidly during the favorable growing season (Ray, Botha and Chinsamy, 2004; Botha-Brink and
472 Angielczyk, 2010; Huttenlocker and Botha-Brink, 2014). These animals may have been capable
473 of heterothermic endothermy (the use of metabolic heat to increase body temperature), where
474 basal metabolic rates (BMR) increased beyond that of ectotherms during bouts of activity
475 (Hopson, 2012) or seasonally during warmer periods (Angilletta et al., 2010). Pörtner (2004)
476 even suggested that it was adaptation to cold eurythermy (the ability to withstand a wide range of
477 ambient temperatures, but specifically in environments with a low mean temperature) as early as

478 the early–middle Permian that selected for improved mitochondrial capacity and increased
479 densities (i.e. increased membrane leakiness where extra protons not taken up in ATP synthesis
480 dissipate free energy as heat). Mitochondria function more efficiently at higher temperatures and
481 a warm body would have improved mitochondrial efficiency (Clarke and Pörtner, 2010). The
482 plasma membranes of extant endothermic mammalian and avian cells also generate heat while
483 attempting to maintain their sodium–potassium ion gradients, although this comes at a great
484 metabolic cost compared to ectotherms (Hillenius and Ruben, 2004).

485 Yet, Hillenius and Ruben (2004) have argued that if leaky membranes evolved for
486 endogenous heat production then endotherms should devote a larger quantity of total cellular
487 metabolism to maintaining the ion gradient compared to ectotherms. Experiments on liver and
488 kidney cells, however, have shown that ectotherms and endotherms devote similar proportions of
489 total tissue oxygen consumption to this process. Hillenius and Ruben (2004) suggested instead
490 that increased mitochondrial densities arose for increased aerobic capacity (the aerobic capacity
491 model) and thermogenesis during ion gradient maintenance more likely arose as a metabolic cost
492 rather than as a selecting factor in the evolution of endothermy (Hillenius and Ruben, 2004).

493 There is evidence of elevated growth rates (i.e. higher than those of extant reptiles) in
494 some "pelycosaurs" (basal non-therapsid synapsids), such as *Ophiacodon*, as seen by the
495 presence of well-vascularized fibrolamellar bone tissues in the limb bones of this taxon (Laurin
496 and Buffrénil, 2015; Shelton and Sander, 2017). Lesser amounts of fibrolamellar bone have also
497 been found in sphenacodontid bones (Huttenlocker and Rega, 2012). In extant reptiles,
498 fibrolamellar bone has only been found sporadically in juvenile crocodilians (and recent research
499 suggests that this reptilian lineage likely descended from endothermic ancestors; Legendre et al.,
500 2016). The presence of highly vascularized fibrolamellar bone in "pelycosaurs" is not

widespread, however, with most exhibiting a predominance of slower forming parallel-fibered and lamellar bone (Huttenlocker and Rega, 2012). It is unlikely that "pelycosaurs" had elevated BMR as the associated skeletal structures required for increased aerobic capacity to maintain high BMR (e.g. improved ventilation, locomotor and masticatory features necessary for increased energy assimilation, which is crucial to maintaining an elevated metabolic rate) essentially only appeared in the more derived therapsids (Kemp, 2005). However, it does indicate that a departure from the typical poikilothermic ectothermy, such as that seen in extant reptiles, had possibly occurred by this time.

Although non-mammaliaform cynodonts grew in a similar manner to other Late Permian therapsids (as shown by *Procynosuchus*; Botha-Brink, Abdala and Chinsamy, 2012), they remained relatively rare components of the terrestrial ecosystem until after the Permo-Triassic mass extinction event. The following Early Triassic is characterized by a marked decrease in atmospheric oxygen levels and an increase in aridity and temperature extremes (Smith and Botha-Brink, 2014; Rey et al., 2016; MacLeod, Quinton and Bassett, 2017). Most of the therapsids were small and show evidence of burrowing (e.g., Cluver, 1978; Damiani et al., 2003; Botha-Brink et al., 2016; Botha-Brink, 2017). This lifestyle may have provided a thermoregulatory advantage by preventing substantial variations in body temperature during the hot days or cold nights (Fig. 5(1)). Fossoriality appears to have been retained in Middle Triassic to Jurassic non-mammaliaform cynodonts as evidence of burrowing has been found in the gomphodont *Trirachodon* (Groenewald, Welman and MacEachern, 2001) and possibly in the more derived traversodontids and chiniquodontids (Fiorelli et al., 2018), and burrows likely excavated by non-mammaliaform cynodonts have been found in the Lower Jurassic Elliot Formation of South Africa (Bordy et al., 2017).

524 Improved ventilation structures would also have been advantageous in a relatively
525 hypoxic environment (both in the open-air and within burrows). Although atmospheric oxygen
526 levels had begun to decrease during the Late Permian, they dropped considerably following the
527 Permo-Triassic mass extinction (Berner, 2005) and likely had substantial effects on the
528 physiology of the survivors. Early Triassic basal cynodonts, such as *Galesaurus* and
529 *Thrinaxodon*, had bony secondary palates, which, although not selected for endothermy (as they
530 were more likely selected for bite strength as in dicynodonts and therocephalians; Thomason and
531 Russell, 1986), would have allowed them to eat and breathe simultaneously allowing more
532 continuous ventilation to take place (Bennett and Ruben, 1986). They also had enlarged nasal
533 chambers inherited from their Permian ancestors (Fig. 5(2)), which likely housed cartilaginous
534 respiratory turbinates (Crompton et al., 2017). These structures would have been beneficial
535 during this time as they condition the air during respiration. They are crucial for mammalian
536 homeothermic endothermy (Ruben et al., 2012). During inhalation the air is warmed and
537 saturated before entering the lungs via membranes lying on the surface of the maxilloturbinate
538 bones. Upon exhalation water is reabsorbed via these membranes, thus reducing water loss. This
539 adaptation prevents animals with high ventilation rates (i.e. homeothermic endotherms) from
540 dehydrating. They also help to conserve heat because the palatopharyngeus muscle (involved in
541 swallowing, breathing and suckling) holds the larynx in an intranarial position separating the
542 nasal and oral cavities and allowing both inspiration and expiration to occur solely through the
543 nose (Crompton, Musinsky and Owerkowicz, 2015; Crompton et al., 2017). Given the high
544 energetic costs of maintaining a constant body temperature in endotherms, this is an important
545 process for conserving heat in cold ambient temperatures. Respiratory turbinates may also help
546 to dissipate heat in hot environments or during exercise, again helping to maintain constant body

547 temperatures in endotherms (Hillenius, 1992). In extant mammals, heat is dissipated via panting
548 where air is exhaled through the mouth bypassing the turbinates completely. This is achieved by
549 withdrawing the larynx from the nasopharynx using the palatopharyngeus muscle (Crompton,
550 2016; Crompton, Musinsky and Owerkowicz, 2015; Crompton et al., 2017).

551 Ridges in the expected position of maxilloturbinate bones have been reported for the Late
552 Permian therocephalian *Glanosuchus*, the Middle and Late Triassic gomphodonts *Trirachodon*
553 and *Massetognathus* (Hillenius, 1994; Hillenius and Ruben, 2004), as well as the Late Triassic
554 brasilodontid *Brasilitherium* (Ruf et al., 2014). They have also been reported in two specimens
555 of the Early Triassic *Thrinaxodon*, although the ridges are less pronounced than in the
556 gomphodonts (Hillenius, 1994). However, the interpretation of these structures has been
557 questioned (e.g. Kemp, 2006) and recent computed tomography scanning of the nasal region of
558 several Late Triassic non-mammaliaform cynodonts (*Massetognathus*, *Probainognathus*,
559 *Elliotherium*) cannot confirm the presence of maxilloturbinate ridges (Crompton et al., 2017).
560 The structure of the non-mammaliaform nasal region underwent little modification during the
561 Triassic, but the presence of enlarged respiratory chambers suggests that they were filled with
562 cartilaginous respiratory turbinals. Crompton et al. (2017) propose that the initial role of
563 respiratory turbinates in the Early Triassic non-mammaliaform cynodonts was heat dissipation
564 and not water and heat conservation and given the increased ambient temperatures at this time,
565 this function would have been advantageous to those living then and throughout much of the
566 Triassic. These authors suggest that a palatopharyngeus muscle, which would have forced air to
567 pass solely through the nasal region, only evolved in the Late Triassic tritheledontids
568 (*Elliotherium*) and mammaliaforms (*Morganucodon*) and that respiratory turbinates only acted as

569 an efficient heat exchange in the earliest mammals when they became fully ossified, only then
570 allowing for elevated basal and maximum metabolic rates (Crompton et al., 2017).
571 It is unlikely that Early Triassic non-mammaliaform cynodonts had significantly elevated
572 BMR (i.e. similar to that of extant homeothermic endotherms) as their burrowing lifestyle may
573 have limited such a condition. Extant burrowing mammals have lower BMR than non-fossorial
574 species, which is likely related to this lifestyle as it is thought to prevent over-heating while
575 within burrows (McNab, 2012). Additionally McNab and Morrison (1963) and Lovegrove
576 (2000) have demonstrated that mammals living in environments with unpredictable resource
577 availability and rainfall (such as that during the post-extinction Early Triassic) tend to have lower
578 BMR to reduce energy expenditure. However, the burrowing lifestyle may have aided in
579 facultative homeothermy in keeping body temperatures constant.
580 The recovery of a juvenile (skull length 40% of adult BSL) with two adult specimens of
581 the Middle Triassic *Trirachodon* within a burrow (NMQR 3281; Groenewald, Welman and
582 MacEachern, 2001) strongly suggests that some form of extended parental care had evolved by
583 this time (Fig. 5(3)). Farmer (2000) proposed that endothermy evolved due to a selection for
584 increased thermogenesis in pregnant females, which allowed them to control incubation
585 temperature. Embryos growing at higher temperatures benefit by incurring fewer developmental
586 abnormalities and exhibiting increased survival rates. Parental thermogenesis extending to
587 include neonates would have increased their survival rate as well (Farmer, 2000). Support for
588 this hypothesis is found in the echidna (Grigg, Beard and Augee, 2004) and more recently in tegu
589 lizards that exhibit elevated body temperatures during the reproductive phase (Tattersall, 2016).
590 Thus, improved locomotory, masticatory and ventilatory structures, combined with the
591 loss of the pineal foramen (Fig. 5(4)) in the lineage leading to the Probainognathia (indicating

592 improved thermoregulatory control and reproductive timing; Benoit et al., 2016a) and the
593 possible presence of maxillary vibrissae (i.e. whiskers) (Fig. 5(5)) within the prozostrodontian
594 lineage, indicating that hair (perhaps not a pelage) had evolved to some extent by this time
595 (Benoit, Manger and Rubidge, 2016b), as well as the possible evolution of extended parental
596 care by this stage, shows that there was a progressive increase in the acquisition of physiological
597 mammalian features during the Middle–Late Triassic. These changes are mirrored in the
598 osteohistology of the Prozostrodontia, which exhibit high growth rates, despite smaller body
599 sizes.

600 However, despite the brasilodontids being similar in size to small extant mammals that
601 typically reach reproductive maturity within one year (Miller and Zammuto, 1983; Promislow
602 and Harvey, 1990), these animals still took more than one year to reach growth attenuation.
603 Thus, although the Early Triassic non-mammaliaform cynodonts matured within one year
604 (Botha-Brink et al., 2016), this ability was lost when the lineage diverged into larger body sizes
605 during the Middle Triassic and took a relatively long time to be regained. The relatively more
606 protracted growth period of the brasilodontids suggests that they had yet to attain the truncated
607 growth period postulated for *Morganucodon* (Fig. 5(6)), that which is typical of extant placental
608 mammals of similar body size (O'Meara and Asher, 2016).

609 As evidence of ossified maxilloturbinate bones has only been found in the Late Triassic
610 tritheledontids and mammaliaforms (Fig. 5(7)), it is likely that high, mammalian-type,
611 ventilation rates were only possible within these clades. However, many of the physiological and
612 behavioral attributes necessary for homeothermic endothermy had appeared by this time, making
613 significantly elevated maximum and basal metabolic rates possible.

614

CONCLUSIONS

The osteohistological assessment of several prozostrodontian cynodont taxa from basal to more derived forms indicates the presence of high growth rates, similar to other non-mammaliaform cynodonts. Rapid early growth with annual interruptions later in ontogeny is clearly observed in *Prozostrodon*, the most basal prozostrodontian, and in the tritheledontid *Irajatherium*. *Brasilodon* and *Brasilitherium*, which are currently considered to be the sister taxa to Mammaliaformes, grew more slowly than the less derived cynodonts and more similarly to the mammaliaform *Morganucodon* and the multituberculates *Kryptobaatar* and *Nemegtbaatar*. The slower growth rates in these brasilodontids compared to other non-mammaliaform cynodonts may be related to phylogeny and/or decreased body sizes as all these taxa were very small. When compared with similar-sized extant mammals, they may have grown more slowly to adult size as their osteohistology shows it took more than one year for growth to attenuate, thus taking more than one year for these animals to reach somatic maturity. Thus, although the Prozostrodontia exhibit increasingly mammalian characteristics, including rapid juvenile growth, the small derived prozostrodontians still exhibit an extended growth period compared to similar-sized extant mammals.

REFERENCES

Abdala F. 2007. Redescription of *Platycraniellus elegans* (Therapsida, Cynodontia) from the Lower Triassic of South Africa, and the cladistic relationships of eutheriodonts. *Palaeontology* 50:591–618.

636 Abdala F, Ribeiro AM. 2010. Distribution and diversity patterns of Triassic cynodonts
637 (Therapsida, Cynodontia) in Gondwana. *Palaeogeography, Palaeoclimatology,*
638 *Palaeoecology* 286:202–217.
639 Angilletta MJ Jr, Cooper BS, Schuler MS, Boyles JG. 2010. The evolution of thermal physiology
640 in endotherms. *Frontiers in Bioscience* E2:828–881.
641 Bennett AF, Ruben JA. 1986. The metabolic and thermoregulatory status of therapsids. In:
642 Hotton III N, MacLean PD, Roth JJ, Roth EC, eds. *The ecology and biology of mammal-like*
643 *reptiles*. Washington DC: Smithsonian Institution Press, 207–218.
644 Benoit J, Abdala F, Manger PR, Rubidge BS. 2016a. The sixth sense in mammalians
645 forerunners: Variability of the parietal foramen and the evolution of the pineal eye in South
646 African Permo-Triassic eutheriodont therapsids. *Acta Palaeontologica Polonica* 61:777–
647 789.
648 Benoit J, Manger PR, Rubidge BS. 2016b. Palaeoneurological clues to the evolution of defining
649 mammalian soft tissue traits. *Scientific Reports* 6:25604.
650 Berner RA. 2005. The carbon and sulfur cycles and atmospheric oxygen from middle Permian to
651 middle Triassic. *Geochimica et Cosmochimica Acta* 69:3211–3217.
652 Bonaparte JF. 2013. Evolution of the Brasilodontidae (Cynodontia-Eucynodontia). *Historical*
653 *Biology* 25:643–653.
654 Bonaparte JF, Barberena MC. 2001. On two advanced carnivorous cynodonts from the Late
655 Triassic of Southern Brazil. *Bulletin of the Museum of Comparative Zoology at Harvard*
656 156:59–80.

Bonaparte JF, Martinelli AG, Schultz CL, Rubert R. 2003. The sister group of mammals: small cynodonts from the Late Triassic of southern Brazil. *Revista Brasileira Paleontologia* 5:5–27.

Bonaparte JF, Martinelli AG, Schultz CL. 2005. New information on *Brasilodon* and *Brasilitherium* (Cynodontia, Probainognathia) from the Late Triassic of southern Brazil. *Revista Brasileira Paleontologia* 8:25–46.

Bonaparte JF, Schultz CL, Soares MB, Martinelli AG. 2010. La fauna local de Faxinal do Soturno, Triásico Tardío de Rio Grande do Sul, Brasil. *Revista Brasileira de Paleontologia* 13:233–246.

Bonaparte JF, Soares M, Martinelli AG. 2012. Discoveries in the Late Triassic of Brazil improve knowledge on the origin of mammals. *Historia Natural, Fundación Felix de Azara, Tercera Serie* 2012:5–30.

Botha J, Chinsamy A. 2000. Growth patterns deduced from the histology of the cynodonts *Diademodon* and *Cynognathus*. *Journal of Vertebrate Paleontology* 20:705–711.

Botha J, Chinsamy A. 2004. Growth and life habits of the Triassic cynodont *Trirachodon*, inferred from bone histology. *Acta Paleontologica Polonica* 49:619–627.

Botha-Brink J. 2017. Burrowing in *Lystrosaurus*: preadaptation to a postextinction environment? *Journal of Vertebrate Paleontology* 37: e1365080. DOI: 10.1080/02724634.2017.1365080.

Botha-Brink J, Angielczyk KD. 2010. Do extraordinarily high growth rates in Permo-Triassic dicynodonts (Therapsida, Anomodontia) explain their success before and after the end-Permian extinction? *Zoological Journal of the Linnean Society* 160:341–365.

678 Botha-Brink J, Abdala F, Chinsamy A. 2012. The radiation and osteohistology of non-
679 mammaliaform cynodonts. In: Chinsamy-Turan A, ed. F*orerunners of mammals: radiation,*
680 *histology, biology*. Bloomington: Indiana University Press, 223–246.
681 Botha-Brink J, Huttenlocker A, Angielczyk KD, Codron D, Ruta M. 2016. Breeding young as a
682 survival strategy during Earth's greatest mass extinction. *Scientific Reports* 6: 24053. DOI:
683 10.1038/srep24053.
684 Bordy E, Sciscio L, Abdala F, Mcphee B, Choiniere J. 2017. First Lower Jurassic vertebrate
685 burrow from southern Africa (upper Elliot Formation, Karoo Basin, South Africa).
686 *Palaeogeography, Palaeoclimatology, Palaeoecology* 468:362–372.
687 Case TJ. 1978. Speculations on the growth rate and reproduction of some dinosaurs.
688 *Paleobiology* 4:320–328.
689 Castanet J, Croci S, Aujard F, Perret M, Cubo J, Margerie de E. 2004. Lines of arrested growth
690 in bone and age estimation in a small primate: *Microcebus murinus*. *Journal of Zoology*
691 263:31–39.
692 Chinsamy A, Abdala NF. 2008. Paleobiological implications of the bone microstructure of South
693 American traversodontids (Therapsida: Cynodontia). *South African Journal of Science*
694 104:225–230.
695 Chinsamy A, Hurum JH. 2006. Bone microstructure and growth patterns of early mammals. *Acta*
696 *Palaeontologica Polonica* 51:325–338.
697 Clark JM, Hopson JA. 1985. Distinctive mammal-like reptile from Mexico and its bearing on the
698 phylogeny of the Tritylodontidae. *Nature* 315:398–400.
699 Clarke A, Pörtner HO. 2010. Temperature, metabolic power and the evolution of endothermy.
700 *Biological Reviews* 85:703–727.

701 Cluver MA. 1978. The skeleton of the mammal-like reptile *Cistecephalus* with evidence for a
702 fossorial mode of life. *Annals of the South African Museum* 76:213–246.
703 Crompton AW. 2016. Origin of the dual function of respiratory turbinates in mammals. Journal
704 of Vertebrate Paleontology, SVP Program and Abstracts Book, 2016:122.
705 Crompton AW, Musinsky C, Owerkowicz T. 2015. Evolution of the mammalian nose. In: Dial
706 K, Shubin, N, Brainerd E, eds. *Great transformations in vertebrate evolution*. Chicago:
707 University of Chicago Press, 189–203.
708 Crompton AW, Owerkowicz T, Bhullar B-AS, Musinsky C. 2017. Structure of the nasal region
709 of non-mammalian cynodonts and mammaliaforms: speculations on the evolution of
710 mammalian endothermy. *Journal of Vertebrate Paleontology* e1269116. DOI:
711 10.1080/02724634.2017.1269116.
712 Damiani R, Modesto S, Yates A, Neveling J. 2003. Earliest evidence of cynodont burrowing.
713 *Proceedings of the Royal Society B* 270:1747–1751.
714 Farmer CG. 2000. The key to understanding endothermy and other convergent features in birds
715 and mammals. *The American Naturalist* 155:326–334.
716 Fiorelli LE, Rocher S, Martinelli AG, Ezcurra MD, Hechenleitner EM, Ezpeleta M. 2018.
717 Tetrapod burrows from the Middle–Upper Triassic Chanares Formation (La Rioja,
718 Argentina) and its palaeoecological implications. *Palaeogeography, Palaeoclimatology,*
719 *Palaeoecology*. DOI: 10.1016/j.palaeo.2018.01.026
720 Francillon-Vieillot H, Buffrénil de V, Castanet J, Geraudie J, Meunier FJ, Sire JY, Zylberberg L,
721 Ricqlès de A. 1990. Microstructure and mineralization of vertebrate skeletal tissues. In:
722 Carter JG, ed. *Skeletal Biomineralization: Patterns, Processes and Evolutionary Trends*.
723 New York: Van Nestrand Reinhold, 471–548.

724 Gaetano LC, Abdala F, Govender R. 2017. The postcranial skeleton of the Lower Jurassic
725 *Tritylodon longaevus* from southern Africa. *Ameghiniana* 54(1):1–35.
726 Gow CE. 1980. The dentitions of the Tritheledontidae (Therapsida: Cynodontia). *Proceedings of*
727 *the Royal Society of London B* 208:461–481.
728 Gradstein FM, Ogg JG, Hilgen FJ. 2012. On the geologic time scale. *Newsletters on Stratigraphy*
729 45:171–188.
730 Grigg GC, Beard LA, Augee ML. 2004. The evolution of endothermy and its diversity in
731 mammals and birds. *Physiological and Biochemical Zoology* 77:982–997.
732 Groenewald GH, Welman J, MacEachern JA. 2001. Vertebrate burrow complexes from the Early
733 Triassic *Cynognathus* Zone (Driekoppen Formation, Beaufort Group) of the Karoo Basin,
734 South Africa. *Palaios* 16:148–160.
735 Hillenius WH. 1992. The evolution of nasal turbinates and mammalian endothermy.
736 *Paleobiology* 18:7–29.
737 Hillenius WH. 1994. Turbinates in therapsids: evidence for Late Permian origins of mammalian
738 endothermy. *Evolution* 48:207–229.
739 Hillenius WH, Ruben JA. 2004. The evolution of endothermy in terrestrial vertebrates: Who?
740 When? Why? *Physiological and Biochemical Zoology* 77:1019–1042.
741 Hopson JA. 2012. The role of foraging mode in the origin of therapsids: Implications for the
742 origin of mammalian endothermy. *Fieldiana Life and Earth Sciences* 5:126–148.
743 Hopson JA, Kitching JW. 2001. A probainognathian cynodont from South Africa and the
744 phylogeny of nonmammalian cynodonts. *Bulletin of the Museum of Comparative Zoology*
745 156:5–35.

746 Horn BLD, Melo TM, Schultz CL, Philipp RP, Kloss HP, Goldberg K. 2014. A new third-order
747 sequence stratigraphic framework applied to the Triassic of the Paraná Basin, Rio Grande do
748 Sul, Brazil, based on structural, stratigraphic and paleontological data. *Journal of South*
749 *American Earth Sciences* 55:123–132.
750 Huttenlocker AK, Botha-Brink J. 2014. Growth Patterns and the Evolution of Bone
751 Microstructure in Permo-Triassic Therocephalians (Amniota, Therapsida) of South Africa.
752 *PeerJ* 2:e325. DOI: 10.7717/peerj.325.
753 Huttenlocker AK, Rega E. 2012. The paleobiology and bone microstructure of pelycosaurian-
754 grade synapsids. In: Chinsamy-Turan A, ed. F*orerunners of mammals: radiation, histology,*
755 *biology*. Bloomington: Indiana University Press, 90–119.
756 Jenkins FA. 1971. The postcranial skeleton of African cynodonts. *Bulletin Peabody Museum of*
757 *Natural History*, Yale University 36:1–216.
758 Kemp TS. 2005. *The origin and evolution of mammals*. Oxford: Oxford University Press.
759 Kemp TS. 2006. The origin of mammalian endothermy: a paradigm for the evolution of complex
760 biological structure. *Zoological Journal of the Linnean Society* 147:473–488.
761 Kielan-Jaworowska Z. 1970. New Upper Cretaceous multituberculate genera from Bayn Dzak,
762 Gobi Desert. *Palaeontologica Polonica* 21:35–49.
763 Kielan-Jaworowska Z. 1974. Multituberculate succession in the Late Cretaceous of
764 the Gobi Desert (Mongolia). *Palaeontologica Polonica* 30:23–44.
765 Kielan-Jaworowska Z, Cifelli CL, Luo ZX. 2004. *Mammals from the age of dinosaurs*. New
766 York: New York University Press.
767 Köhler M, Marín-Moratalla N, Jordana X, Aanes R. 2012. Seasonal bone growth and physiology
768 in endotherms shed light on dinosaur physiology. *Nature* 487:358–361.

769 Langer MC. 2005. Studies on continental Late Triassic tetrapod biochronology. II. The
770 Ischigualastian and a Carnian global correlation. *Journal of South American Earth Sciences*
771 19:219–239.
772 Laurin M, Buffrénil de V. 2015. Microstructural features of the femur in early ophiacodontids: A
773 reappraisal of ancestral habitat use and lifestyle in amniotes. *Comptes Rendus Palevol*
774 15:119–131.
775 Lee AH, Werning S. 2008. Sexual maturity in growing dinosaurs does not fit reptilian growth
776 models. *Proceedings of the National Academy of Sciences U S A Biological Sciences*
777 105:582–587.
778 Legendre LJ, Guénard G, Botha-Brink J, Cubo J. 2016. Palaeohistological evidence for ancestral
779 endothermy in archosaurs. *Systematic Biology* DOI: 10.1093/sysbio/syw033.
780 Liu J, Olsen PE. 2010. The phylogenetic relationships of Eucynodontia (Amniota, Synapsida).
781 *Journal of Mammalian Evolution* 17:151–176.
782 Lovegrove BG. 2000. The zoogeography of mammalian basal metabolic rate. *The American*
783 *Naturalist* 156:201–219.
784 Luo Z-X. 1994. Sister-group relationships of mammals and transformations of diagnostic
785 mammalian characters. In: Fraser NC, Sues H-D, eds. *In the Shadow of the Dinosaurs*.
786 Cambridge: Cambridge University Press, 98–128.
787 Luo Z-X, Crompton AW, Sun A-L. 2001. A new mammaliaform from the Early Jurassic and
788 evolution of mammalian characteristics *Science* 292:1535–1540.
789 MacLeod KG, Quinton PC, Bassett DJ. 2017 Warming and increased aridity during the earliest
790 Triassic in the Karoo Basin, South Africa. *Geology* 45:483–486.

Magwene PM. 1993. What's bred in the bone: histology and cross-sectional geometry of mammal-like reptile long bones-evidence of changing physiological and biomechanical demands. M.S. Thesis, Harvard University.

Martínez R, Apaldetti C, Alcober OA, Colombi CE, Sereno PC, Fernández E, Santi Malnis P, Correa GA, Abelín D. 2013. Vertebrate succession in the Ischigualasto Formation. Society of Vertebrate Paleontology Memoir 12, *Journal of Vertebrate Paleontology* 32:10–30.

Martinelli AG. 2017. Contribuição ao conhecimento dos cinodontes probainognátios (Therapsida, Cynodontia, Probainognathia) do Triássico da América do Sul e seu impacto na origem dos Mammaliaformes. D. Phil. Universidade Federal do Rio Grande do Sul.

Martinelli AG, Bento Soares M, Schwanke C. 2016. Two new cynodonts (Therapsida) from the Middle-Early Late Triassic of Brazil and comments on South American probainognathians. *PLoS ONE* 11:e0162945.

Martinelli AG, Bonaparte JF. 2011. Postcanine replacement in *Brasilodon* and *Brasilitherium* (Cynodontia, Probainognathia) and its bearing in cynodont evolution. In: Calvo J, Porfiri J, González Riga B, Dos Santos D, eds. *Dinosaurios y Paleontología desde América Latina, Anales del III Congreso Latinoamericano de Paleontología (Neuquén, 2008)*. Mendoza: Editorial de la Universidad Nacional de Cuyo, 179–186.

Martinelli AG, Bonaparte JF, Schultz CL, Rubert R. 2005. A new tritheledontid (Therapsida, Eucynodontia) from the Late Triassic of Rio Grande do Sul (Brazil) and its phylogenetic relationships among carnivorous non-mammalian eucynodonts. *Ameghiniana* 42:191–208.

Martinelli AG, Eltink E, Da-Rosa ÁAS, Langer MC. 2017a. A new cynodont (Therapsida) from the *Hyperodapedon* Assemblage Zone (upper Carnian-Norian) of southern Brazil improves the Late Triassic probainognathian diversity. *Papers in Palaeontology* 3:401–423.

814 Martinelli AG, Rougier GW. 2007. On *Chaliminia musteloides* Bonaparte (Cynodontia,
815 Tritheledontidae) and the phylogeny of the Ictidosauria. *Journal of Vertebrate Paleontology*
816 27:442–460.
817 Martinelli AG, Soares MB. 2016. Evolution of South American cynodonts. *Contribuciones del*
818 *Museo Argentino de Ciencias Naturales "Bernardino Rivadavia"* 6:183–197.
819 Martinelli AG, Soares MB, Oliveira TV, Rodrigues PG, Schultz CL. 2017b. The Triassic
820 eucynodont *Candelariodon barberenai* revisited and the early diversity of stem
821 prozostrodontians. *Acta Palaeontologica Polonica* 62:527–542.
822 Matsuoka H, Kusuhashi N, Corfe IJ. 2016. A new Early Cretaceous tritylodontid (Synapsida,
823 Cynodontia, Mammaliamorpha) from the Kuwajima Formation (Tetori Group) of central
824 Japan. *Journal of Vertebrate Paleontology* 36:e1112289.
825 McNab BK. 2012. *Extreme measures. The ecological energetics of birds and mammals*.
826 Chicago: University of Chicago Press.
827 McNab BK, Morrison P. 1963. Body temperature and metabolism in subspecies of *Peromyscus*
828 from arid and mesic environments. *Ecological Monographs* 33:63–82.
829 Miller JS, Zammuto RM. 1983. Life histories of mammals: An analysis of life tables. *Ecology*
830 64:631–635.
831 Nesterenko V, Ohdachi SD. 2001. Postnatal growth and development in *Sorex unguiculatus*.
832 *Mammal Study* 26:145–148.
833 Oliveira TV, Martinelli AG, Bento Soares M. 2011. New material of *Irajatherium hernandezi*
834 Martinelli, Bonaparte, Schultz and Rubert 2005 (Eucynodontia, Tritheledontidae) from the
835 Upper Triassic (Caturrita Formation, Paraná Basin) of Brazil. *Paläontologische Zeitschrift*
836 85:67–82.

837 O'Meara RN, Asher RJ. 2016. The evolution of growth patterns in mammalian versus
838 nonmammalian cynodonts. *Paleobiology* 42:439–464.
839 Owens FN, Dubeski P, Hanson CF. 1993. Factors that alter the growth and development of
840 ruminants. *Journal of Animal Science* 71:3138–3150.
841 Pörtner HO. 2004. Climate variability and the energetic pathways of evolution: The origin of
842 endothermy in mammals and birds. *Physiological and Biochemical Zoology: Ecology and*
843 *Evolutionary Approaches* 77:959–981.
844 Promislow DEL, Harvey PH. 1990. Living fast and dying young: A comparative analysis of life-
845 history variation among mammals. *Journal of Zoology London* 220:417–9437.
846 Ray S, Botha J, Chinsamy A. 2004. Bone histology and growth patterns of some non-
847 mammalian therapsids. *Journal of Vertebrate Paleontology* 24:634–648.
848 Rey K, Amiot R, Fourel F, Rigaudier T, Abdala F, Day MO, Fernandez V, Fluteau F, France-
849 Lanord C, Rubidge BS, Smith RM, Viglietti PA, Zipfel B, Lécuyer C. 2016. Global climate
850 perturbations during the Permo-Triassic mass extinctions recorded by continental tetrapods
851 from South Africa. *Gondwana Research* 37:384–396.
852 Ricqlès de A, Meunier FJ, Castanet J, Francillon-Vieillot H. 1991. Comparative microstructure
853 of bone. In: Hall BK, ed. *Bone, Volume 3: Bone matrix and bone specific products*. Boca
854 Raton: CRC Press. 1–77.
855 Rodrigues PG, Ruf I, Schultz CL. 2013. Digital reconstruction of the otic region and inner ear of
856 the non-mammalian cynodont *Brasilitherium riograndensis* (Late Triassic, Brazil) and its
857 relevance to the evolution of the mammalian ear. *Journal of Mammalian Evolution* 20:291–
858 307.

Rodrigues PG, Ruf I, Schultz CL. 2014. Study of a digital cranial endocast of the non-mammaliaform cynodont *Brasilitherium riograndensis* (Later Triassic, Brazil) and its relevance to the evolution of the mammalian brain. *Paläontologische Zeitschrift* 88:329–352.

Ruben JA, Hillenius WJ, Kemp TS, Quick DE. 2012. The evolution of mammalian endothermy. In: Chinsamy-Turan A, ed. *Forerunners of mammals: radiation, histology, biology*. Bloomington: Indiana University Press, 273–286.

Ruf I, Maier W, Rodrigues PG, Schultz CL. 2014. Nasal anatomy of the non-mammaliaform cynodont *Brasilitherium riograndensis* (Eucynodontia, Therapsida) reveals new insight into mammalian evolution. *The Anatomical Record* 297:2018–2030.

Ruta M, Botha-Brink J, Mitchell SA, Benton MJ. 2013. The radiation of cynodonts and the ground plan of mammalian morphological diversity. *Proceedings of the Royal Society B* 280: 20131865. DOI: 10.1098/rspb.2013.1865.

Shelton CD, Chinsamy A. 2016. Postcranial bone histology of dinocephalians (Therapsida) reveals periodic rapid rates of bone deposition and evidence of a pathology in a titanosuchid. Journal of Vertebrate Paleontology, SVP Program and Abstracts Book, 2016: 223.

Shelton CD, Sander PM. 2017. Long bone histology of *Ophiacodon* reveals the geologically earliest occurrence of fibrolamellar bone in the mammalian stem lineage. *Comptes Rendus Palevol* 16:397–424.

Smith RMH, Botha-Brink J. 2014. Anatomy of an extinction: Sedimentological and taphonomic evidence for drought-induced die-offs during the Permo-Triassic mass extinction in the main Karoo Basin, South Africa. *Palaeogeography, Palaeoclimatology, Palaeoecology* 396:99–118.

882 Soares MB, Martinelli AG, Oliveira TV. 2014. A new prozostrodontian cynodont (Therapsida)
883 from the Late Triassic *Riograndia* Assemblage Zone (Santa Maria Supersequence) of
884 Southern Brazil. *Anais da Academia Brasileira de Ciências* 86:1673–1691.
885 Soares MB, Schultz CL, Horn BLD. 2011. New information on *Riograndia guaibensis*
886 Bonaparte, Ferigolo and Ribeiro, 2001 (Eucynodontia, Tritheledontidae) from the Late
887 Triassic of southern Brazil: anatomical and biostratigraphic implications. *Anais da*
888 *Academia Brasileira de Ciências* 83:329–354.
889 Sues H-D. 1986. The skull and dentition of two tritylodontid synapsids from the Lower Jurassic
890 of western North America. *Bulletin of the Museum of Comparative Zoology* 151:217–268.
891 Stein K, Prondvai E. 2013. Rethinking the nature of fibrolamellar bone: an integrative biological
892 revision of sauropod plexiform bone formation. *Biological Reviews* 89:24–47.
893 Tatttersall GJ. 2016. Reptile thermogenesis and the origins of endothermy. *Zoology* 119:403–
894 405.
895 Thomason JJ, Russell AP. 1986. Mechanical factors in the evolution of the mammalian
896 secondary palate: a theoretical analysis. *Journal of Morphology* 189:199–213.
897 Veiga FH, Botha-Brink J, Soares MB. 2018. Osteohistology of the non-mammaliaform
898 traversodontids *Protuberum cabralense* and *Exaeretodon riograndensis* from southern
899 Brazil. *Historical Biology*. DOI: 10.1080/08912963.2018.1441292.
900 Zerfass H, Lavina EL, Schultz CL, Garcia AJV, Faccini UF, Chemale F Jr. 2003. Sequence
901 stratigraphy of continental Triassic strata of Southernmost Brazil: a contribution to
902 Southwestern Gondwana palaeogeography and palaeoclimate. *Sedimentary Geology*
903 161:85–105.
904

Figure 1

Limb bone osteohistology of *Prozostrodon brasiliensis* UFRGS-PV-248-T.

(A) Whole cross-section of humerus UFRGS-PV-248a-T in CPL showing a relatively thick cortex and two regions of parallel-fibered bone (arrowheads). (B) High magnification of the humerus showing alternating fibrolamellar and parallel-fibered bone. Arrowhead indicates a LAG within the parallel-fibered bone region. (C) Sharpey's fibers (arrows) in the humerus indicating an area of muscle insertion and a LAG (arrowhead) in the mid-cortex. (D) Whole cross-section of femur UFRGS-PV-248b-T showing a relatively thick cortex and a LAG (arrowhead) running through the wide zone of parallel-fibered bone. (E) High magnification of the femur showing alternating fibrolamellar and parallel-fibered bone with an annulus (arrowhead). (F) Peripheral reticular vascular canals in the fibrolamellar bone of the femur. Arrowhead indicates an annulus. (G) Longitudinal section of the femur showing Sharpey's fibers (arrows) indicating an area of muscle insertion. Abbreviations: FLB, fibrolamellar bone; MC, medullary cavity; PFB, parallel-fibered bone. Scale bars equal 100 µm, apart from A and D, which equal 1000 µm.

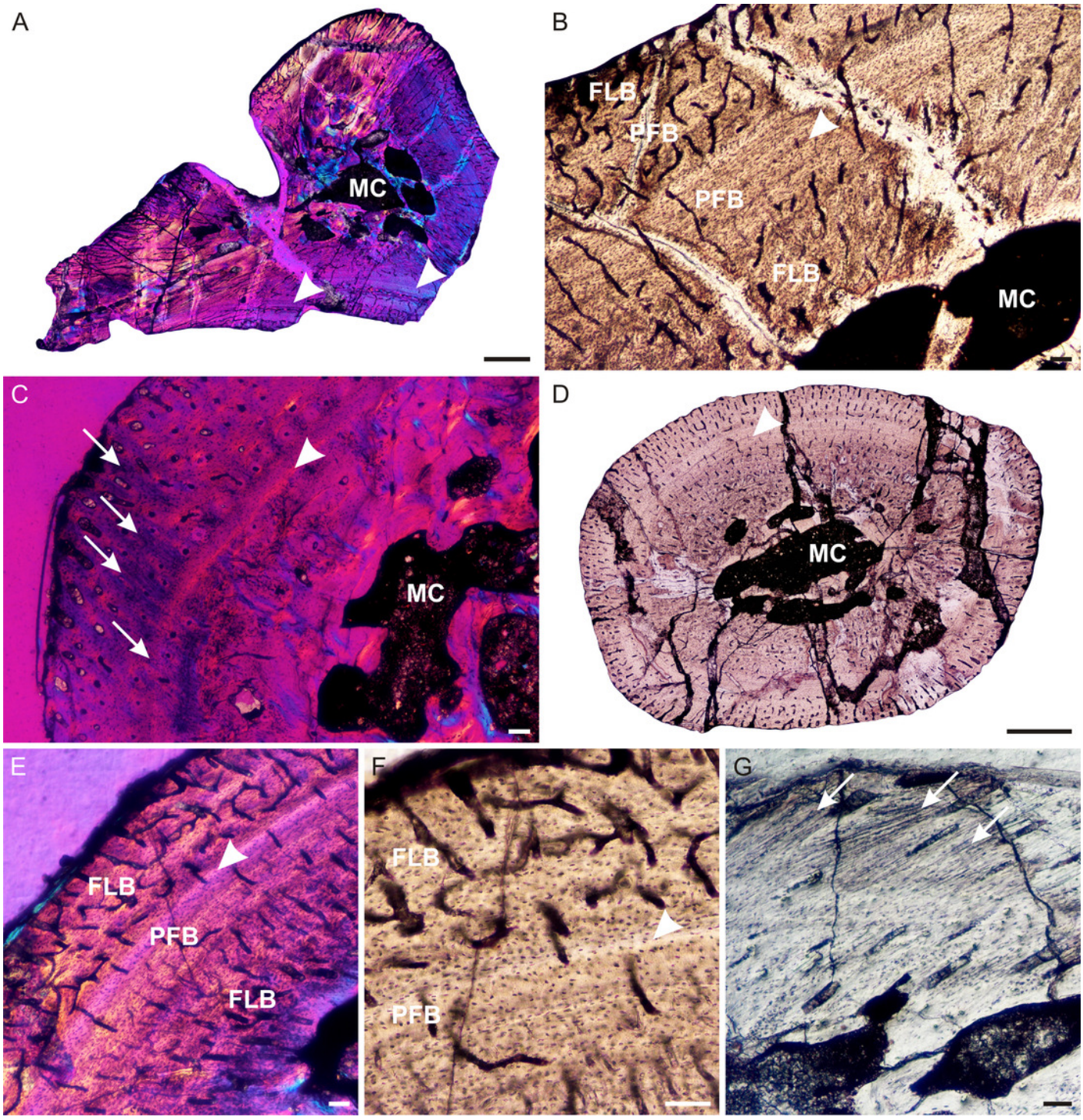
A
MC
B
FLB
PFB
PFB
FLB
MC
C
MC
D
MC
E
FLB
PFB
FLB
F
FLB
PFB
G

Figure 2

Humeral osteohistology of *Irajatherium hernandezi* UFRGS-PV-1072-T.

(A) Whole cross-section showing a relatively thick cortex. A LAG (arrowhead) marks the beginning of a slower growing zone of parallel-fibered and lamellar-zonal bone. (B) Mid-cortical fibrolamellar bone is followed by lamellar-zonal bone with at least one LAG, possibly more (arrowheads). (C) High magnification showing longitudinally-oriented primary osteons in a woven-fibered matrix. (D) Another region of the outer cortex showing lamellar-zonal bone (brackets) with several possible LAGs (arrowheads). Abbreviations: FLB, fibrolamellar bone; LB, lamellar bone; MC, medullary cavity; PFB, parallel-fibered bone. Scale bars equal 100 µm.

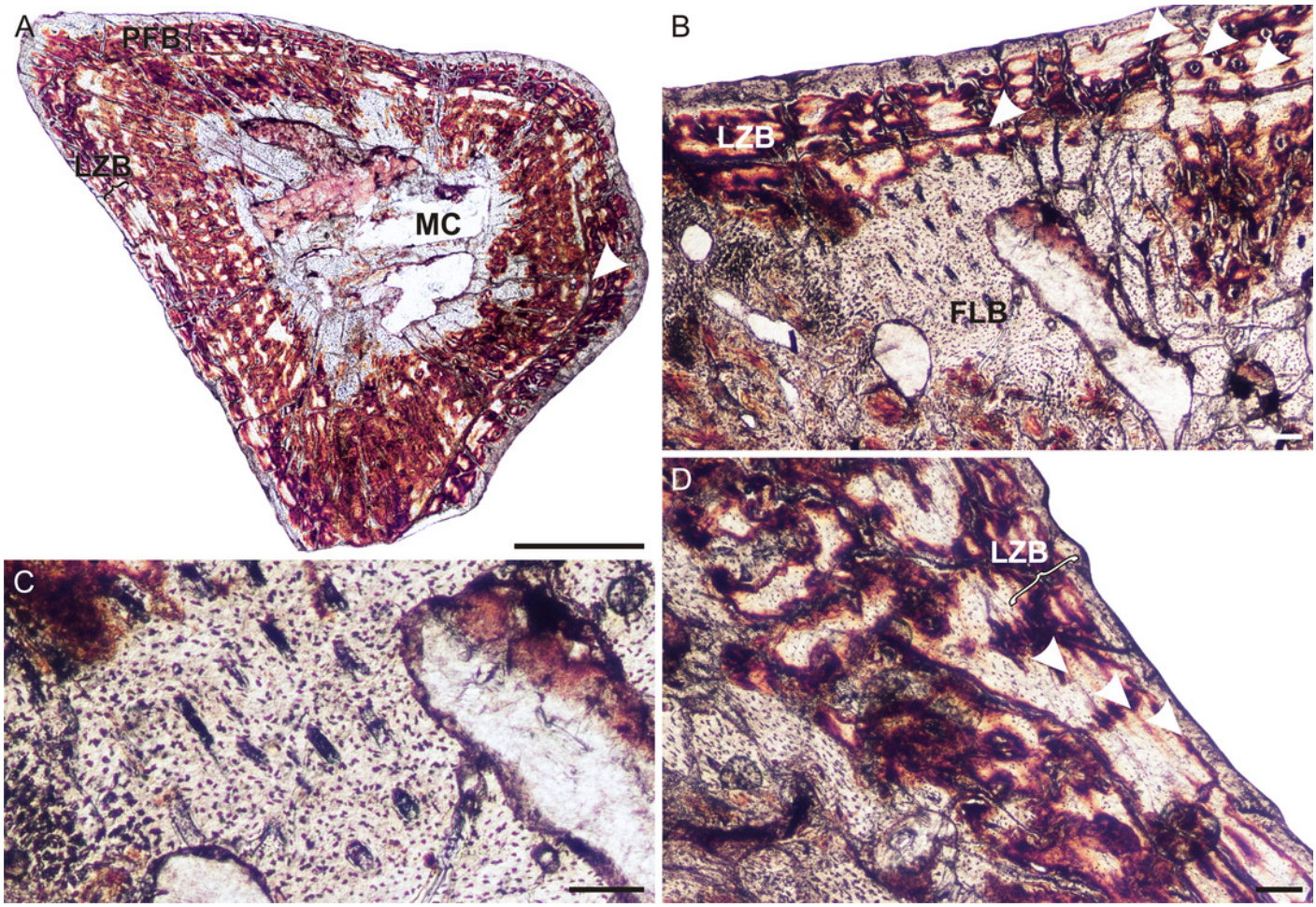

Figure 3

Ulna osteohistology of *Brasilodon quadrangularis* UFRGS-PV-765-T.

(A) Whole cross-section showing a relatively thin cortex. Arrowheads indicate an annulus, arrows indicates secondary osteons. (B) High magnification of woven-fibered bone with several poorly developed primary osteons. (C) Poorly developed fibrolamellar bone in CPL, arrowhead indicates a growth mark. (D) High magnification of the annulus (arrowhead) at the bone periphery. Note the few, flattened osteocyte lacunae within this region. Abbreviations: EB, endosteal bone; PFB, parallel-fibered bone; MC, medullary cavity; WFB, woven-fibered bone. Scale bars = 100 µm.

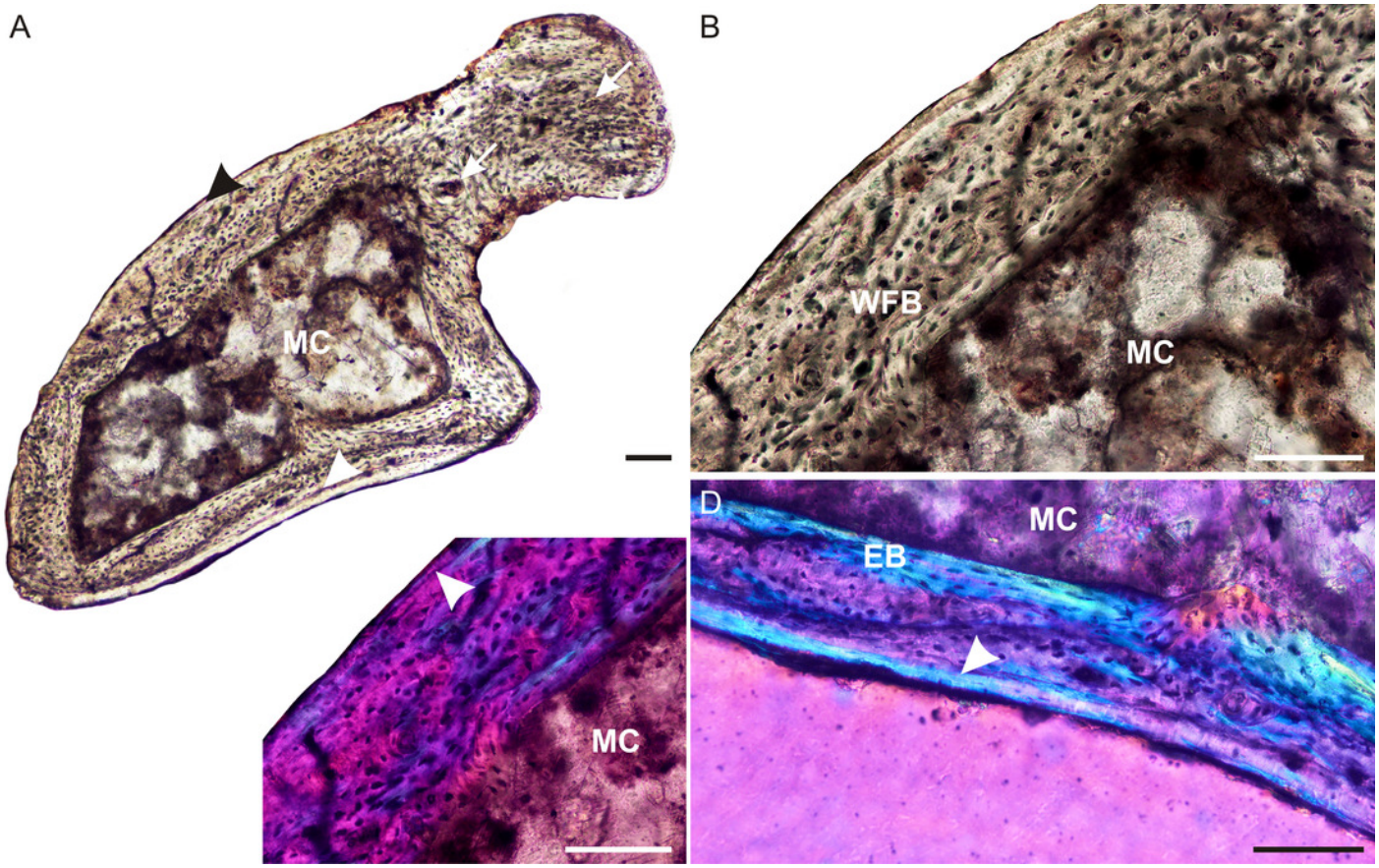

Figure 4

Limb bone osteohistology of *Brasilitherium riograndensis.*

(A) Radius UFRGS-PV-1308a-T showing poorly vascularized parallel-fibered bone tissue. (B) Ulna UFRGS-PV-1308b-T showing lamellar bone. (C) Femur UFRGS-PV-1308c-T showing patches of woven-fibered, parallel-fibered and lamellar bone. (D) High magnification of the femur showing haphazardly arranged osteocyte lacunae (left) and more organized osteocyte lacunae (right). (E) Tibia UFRGS-PV-1308d-T showing patches of woven-fibered and parallel-fibered bone. (F) High magnification of the tibia showing several poorly developed primary osteons (arrows). (G) Fibula UFRGS-PV-1308e-T showing avascular lamellar bone. (H) Femur UFRGS-PV-1043-T in CPL showing a mid-cortical LAG (arrowhead). (I) High magnification of the LAG (arrowhead) followed by slowly forming lamellar bone. (J) High magnification of femur UFRGS-PV-1043-T showing haphazardly arranged osteocyte lacunae and a few small secondary osteons (arrows). Abbreviations: EB, endosteal bone; MC, medullary cavity; PFB, parallel-fibered bone; LB, lamellar bone; WFB, woven-fibered bone. Scale bars = 100 µm.

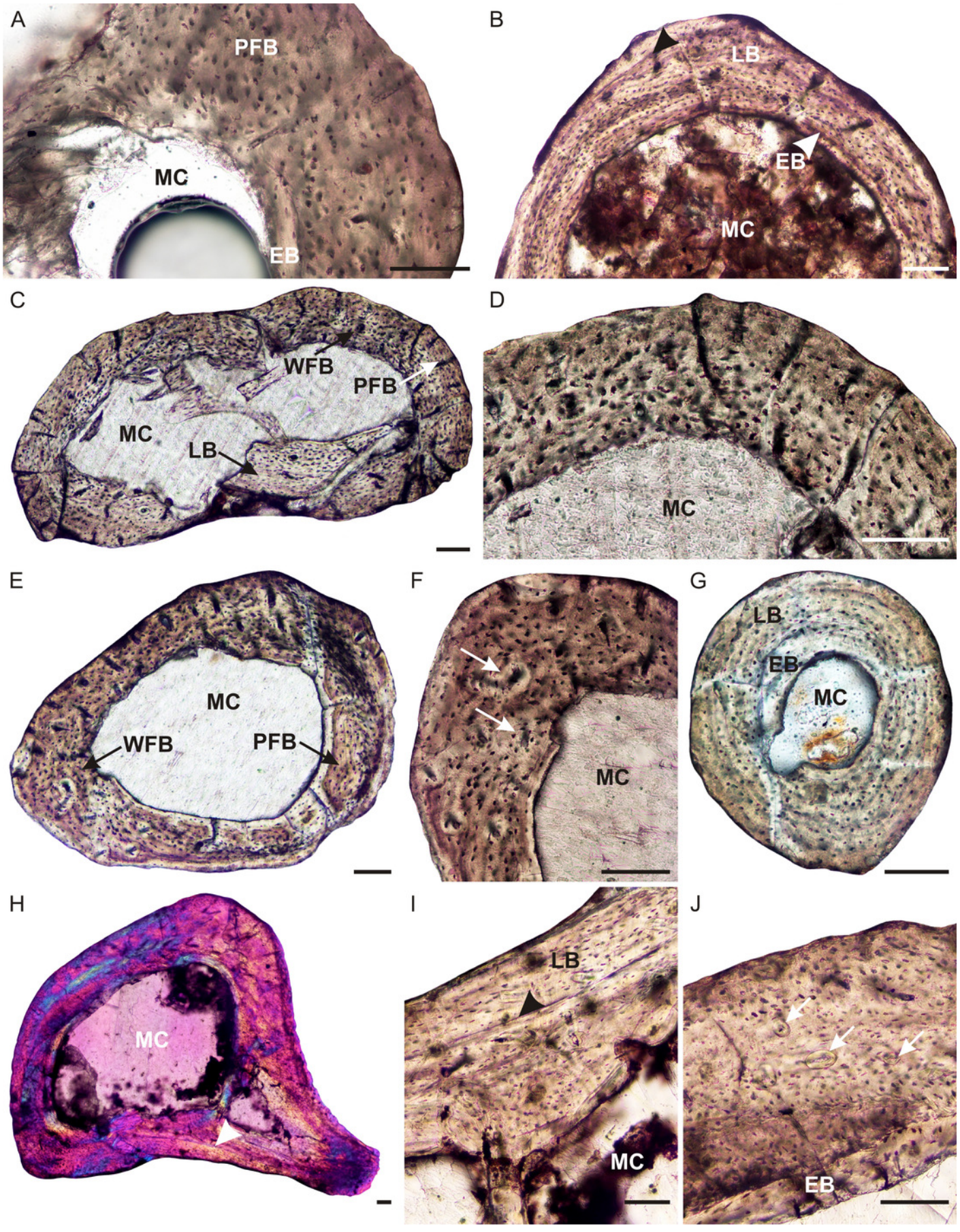
A
PFB
MC
EB
B
LB
EB
MC
C
WFB
PFB
MC
LB
D
MC
E
MC
WFB
PFB
F
MC
G
LB
EB
MC
H
MC
I
LB
MC
J
EB

Figure 5

Life history characteristics mapped onto a Triassic–Jurassic non-mammaliaform cynodont phylogenetic tree.

Growth patterns are known for those taxa shown in white and reveal high growth rates throughout the cynodont lineage. Arrows indicate the possible timing of the evolution of mammalian characteristics for which morphological or behavioral data are known. (1) burrowing, suggesting behavioral thermoregulation, (2) enlarged respiratory chambers inherited from Permian ancestors, which likely housed cartilaginous respiratory turbinates, possibly involved in heat dissipation, (3) extended parental care, suggesting increased parental investment in young, (4) loss of pineal foramen indicating increasing thermoregulatory and reproductive control, (5) possible evolution of maxillary vibrissae indicating improved sensory structures, (6) truncated growth period, similar to small extant mammals, (7) ossified maxillary turbinates indicating efficient counter current exchange system for the conservation of heat and water. Phylogeny taken from Ruta et al. (2013) and Martinelli et al. (2017a, b). Dates taken from Gradstein, Ogg and Hilgen (2012) and Martinelli et al. (2017a, b).

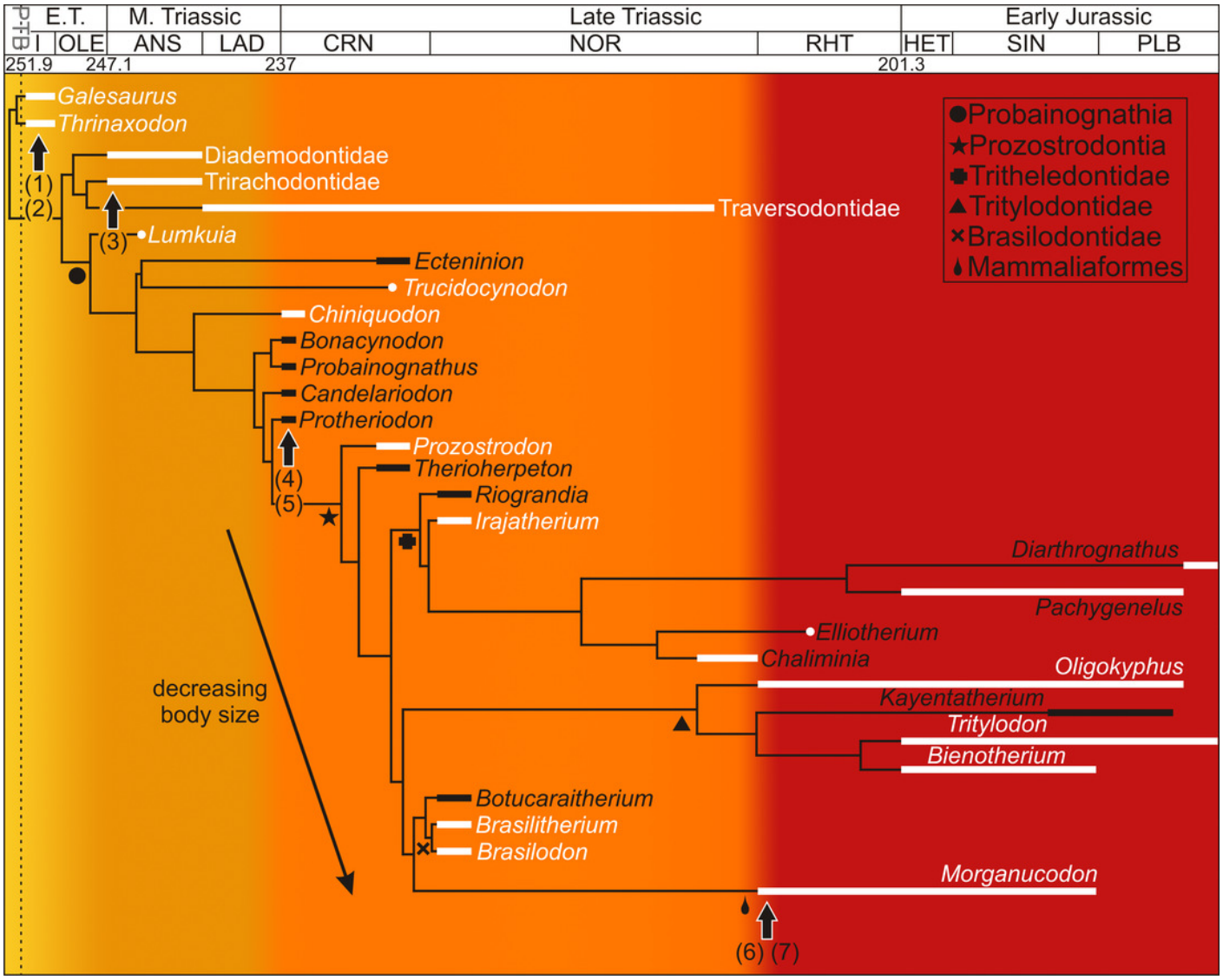
E.T.
M. Triassic
Late Triassic
Early Jurassic
PTB
I
OLE
ANS
LAD
CRN
NOR
RHT
HET
SIN
PLB
251.9
247.1
237
201.3
Galesaurus
Thrinaxodon
(1)
(2)
Diademodontidae
Trirachodontidae
Traversodontidae
(3)
Lumkuia
Ecteninion
Trucidocynodon
Chiniquodon
Bonacynodon
Probainognathus
Candelariodon
Protheriodon
(4)
(5)
Prozostrodon
Therioherpeton
Riograndia
Irajatherium
Diarthrognathus
Pachygenelus
Elliotherium
Chaliminia
Oligokyphus
Kayentatherium
Tritylodon
Bienotherium
Botucaraitherium
Brasilitherium
Brasilodon
Morganucodon
(6) (7)
decreasing
body size
Probainognathia
Prozostrodontia
Tritheledontidae
Tritylodontidae
Brasilodontidae
Mammaliaformes